

# Optical gain in nanocrystalline silicon: comparison of planar waveguide geometry with a non-waveguiding ensemble of nanocrystals

K. Luterová<sup>a,c,\*</sup>, M. Cazzanelli<sup>b</sup>, J.-P. Likforman<sup>c</sup>, D. Navarro<sup>b</sup>,  
J. Valenta<sup>d</sup>, T. Ostatnický<sup>c,d</sup>, K. Dohnalová<sup>a,c</sup>, S. Cheylan<sup>e</sup>, P. Gilliot<sup>c</sup>,  
B. Hönerlage<sup>c</sup>, L. Pavesi<sup>b</sup>, I. Pelant<sup>a</sup>

<sup>a</sup> *Institute of Physics, Academy of Sciences of the Czech Republic, Cukrovarnická 10, 162 53 Praha 6, Czech Republic*

<sup>b</sup> *Dipartimento di Fisica, Università di Trento, via Sommarive 14, 38050 Povo (Trento), Italy*

<sup>c</sup> *Groupe d'Optique Non Linéaire et d'Optoélectronique, IPCMS, Unité mixte CNRS-ULP (UMR 7504),  
23 rue du Loess, B.P. 43, 67034 Strasbourg Cedex 2, France*

<sup>d</sup> *Department of Chemical Physics and Optics, Faculty of Mathematics and Physics, Charles University,  
Ke Karlovu 3, 121 16 Praha 2, Czech Republic*

<sup>e</sup> *Electronic Materials Engineering Department, Research School of Physical Sciences and Engineering, Australian National University,  
Canberra, ACT 0200, Australia*

Available online 12 October 2004

## Abstract

Stimulated emission from nanocrystalline silicon in the visible has become a hot topic during the past years. Various forms of silicon nanostructures are being exploited, among them planar optical waveguides made of silicon nanocrystals, silicon superlattices and tiny silicon nanoparticles. We report on optical gain measurements using the variable-stripe-length and the shifting-excitation-spot methods in two different types of nanocrystalline samples: a planar nanocrystalline waveguide prepared by silicon-ion implantation ( $400\text{ keV}$ ,  $4 \times 10^{17}\text{ cm}^{-2}$ ) into a silica substrate and a layer of porous silicon grains embedded in a sol–gel derived  $\text{SiO}_2$  matrix. The latter does not exhibit any waveguiding. At a first sight one would expect much more favorable conditions for the stimulated emission occurrence in the former type of samples. We observed in fact small optical gain in both types (modal gain of  $12\text{ cm}^{-1}$  at  $\sim 760\text{ nm}$  in ion implanted sample and of  $25\text{ cm}^{-1}$  at  $\sim 650\text{ nm}$  in sol–gel embedded sample, respectively), however, under different pumping conditions. We discuss advantages and disadvantages of both nanostructures, referring in particular to leaky-mode emission that may occur in planar waveguides on transparent substrates.

© 2004 Elsevier B.V. All rights reserved.

## 1. Introduction

Research on light emission from silicon-based materials advanced significantly during the past decade. Various approaches to obtain efficient room temperature

emission were demonstrated, such as atomic layer superlattices, alloying of silicon with germanium or carbon, doping with rare earth atoms, porous silicon, Si nanostructures, molecules or polymers and hybrid methods integrating direct gap materials [1]. Successful build-up of a silicon-based laser represents a main challenge for silicon photonics during these years. An enormous wave of interest in silicon lasing was triggered by the first report on experimental observation of positive optical gain in silicon nanocrystals [2] (Si-nc) prepared

\* Corresponding author. Tel.: +420 220 318 569/+42 2 203 18 414;  
fax: +420 220 318 468.

E-mail address: [luterova@fzu.cz](mailto:luterova@fzu.cz) (K. Luterová).

by Si-ion implantation. The presence of stimulated emission in the red spectral region was later independently confirmed for the Si-nc prepared by various techniques, such as plasma-enhanced chemical vapor deposition [3,4], reactive Si deposition [5], magnetron sputtering [6] and porous silicon embedded in the sol-gel SiO<sub>2</sub> matrix [7]. Stimulated emission has also been achieved in Si nanoclusters emitting in the blue spectral region [8,9].

It appears that not all Si-nc containing samples exhibit optical gain. The requirements for the sample preparation and structure as well as the experimental conditions necessary for reaching stimulated emission have not been fully clarified so far. Most of the investigated samples are designed in the form of a thin Si-nc layer embedded in a transparent silica matrix, or Si/SiO<sub>2</sub> superlattices. Such structures work as asymmetric active planar optical waveguides where the active core layer is formed by the Si-nc layer. Under certain conditions they can show very uncommon photoluminescence (PL) properties [10,11], namely, polarisation resolved narrow spectral modes. The explanation of this effect has been suggested in terms of leaky mode emission propagating along core/substrate boundary [12,13] or, alternatively, as being due to spectral filtering of the waveguide [11]. Moreover, this phenomenon may complicate the interpretation of the experimental data obtained by optical gain measurement [14], together with the difficult full understanding of its possible impact on stimulated emission occurrence.

In this contribution, we compare results of the optical gain measurement by the variable stripe length (VSL) [2–7] technique in two different types of samples—an active planar waveguide made by Si-ion implantation into the silica slab and non-waveguiding ensemble of Si-nc prepared by embedding porous silicon into sol-gel derived SiO<sub>2</sub> matrix. In both structures we observe positive optical gain, however, under different experimental conditions.

## 2. Experimental

Two different types of samples containing Si-nc were used in this study: First, porous silicon grains in sol-gel derived SiO<sub>2</sub> (Por-Si) were prepared by dispersing pulverized porous silicon in phosphorus doped SiO<sub>2</sub> spin-on-glass and subsequent solidification. Full details about the preparation are described elsewhere [7]. The preparation procedure leads to a strongly luminescent layer ( $\sim 1 \times 1 \text{ cm}^2$  with thickness of  $\sim 50 \mu\text{m}$ ) of densely packed Si-nc buried in the SiO<sub>2</sub> matrix (volume concentration of  $\sim 14\%$ ). High Resolution Transmission Electron Microscopy revealed the presence of Si-nc of 2–5 nm in diameter [15]. The active Si-nc layer represents a spontaneous sediment at the cuvette bottom and

owing to irregular surfaces it does not act as a designed planar waveguide. The Por-Si samples were left in the quartz cuvettes to ensure maximal surface flatness during the experiments, while self-supporting samples can also be obtained. Second, the planar waveguide containing Si-nc was prepared by 400 keV Si<sup>+</sup>-ion implantation (a dose of  $4 \times 10^{17} \text{ Si/cm}^2$ ) into a fused silica slab (Infra-sil) with optically polished surface and edges. Subsequent annealing was performed in N<sub>2</sub> atmosphere for 1 h at 1100 °C and then for 1 h in a forming gas (5% H<sub>2</sub> in N<sub>2</sub>) at 500 °C. The presence of Si-nc with diameter of 4–5 nm in the annealed layers was confirmed by Raman scattering.

Optical gain was measured by the standard VSL technique using two different experimental setups employing either femtosecond or nanosecond pulsed pumping. In the femtosecond setup (Strasbourg), excitation pulses ( $\lambda_{\text{exc}} = 395 \text{ nm}$ , duration 100 fs, repetition rate 250 kHz) were delivered by a frequency doubled, regeneratively amplified Ti-sapphire oscillator. The emission from the sample edge was detected by a photomultiplier connected to a lock-in amplifier. The femtosecond VSL configuration was supplemented with the shifting-excitation-spot (SES) measurement [14] ruling out some possible experimental artifacts. The SES measurement replaces the excited stripe by an excited segment created at a variable distance  $x$  from the sample edge. Integration of all SES intensities with respect to the distance  $x$  from the sample edge then yields a curve that basically must show a slight sublinear increase (due to loss) with increasing stripe length, i.e. the sum of all single segment lengths. A VSL curve, on the other hand, represents the emission intensity collected from the whole length of the stripe and it should increase exponentially if positive gain is present.

As for the nanosecond-pumped VSL (Trento), high-fluence pulses (6 ns, 10 Hz, 355 nm) produced by third harmonic of a Nd-YAG laser were used and the time-resolved emission was detected by a single grating spectrometer connected to a picosecond visible streak camera. Signal from the streak camera was integrated over a 90 nm wavelength window. All experiments were performed at room temperature.

## 3. Results

Typical photoluminescence spectrum obtained from Por-Si samples is shown in Fig. 1a. The PL spectrum is broad ( $\sim 280 \text{ nm}$  full width at half maximum—FWHM) and centered at  $\sim 720 \text{ nm}$ , i.e. slightly blue-shifted ( $\sim 20 \text{ nm}$ ) with respect to the PL from the as prepared porous silicon powder used for the sample preparation (drawn as dashed line in Fig. 1a). No spectral change is observed when the PL is collected from the sample edge (in waveguiding geometry).

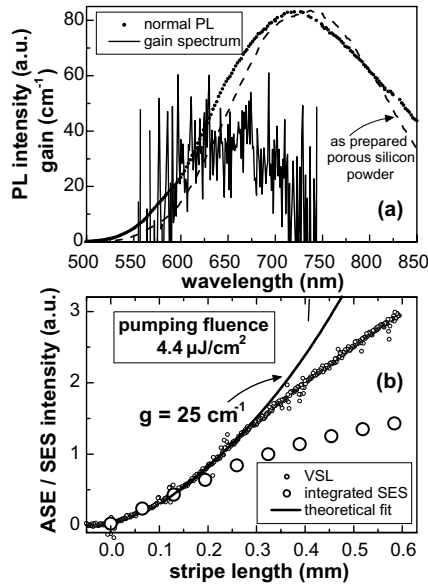


Fig. 1. (a) Normalized normal incidence PL spectrum of the Por-Si sample (dots) excited with a 380nm line of Xe lamp compared to the PL of the as-prepared porous silicon powder (dashed line). Noisy curve: Modal gain spectrum derived from VSL experiment by dividing the emission spectrum recorded at stripe length  $2l$  by the emission spectrum at  $l$ . (b) Femtosecond VSL (small circles) and integrated SES (large circles) curves detected at  $\lambda_{\text{det}} = 670\text{nm}$  and at a pumping fluence of  $4.4\mu\text{J}/\text{cm}^2$ . Full line: theoretical fit of the VSL data according to one-dimensional amplifier model, yielding a positive optical gain  $g = (25 \pm 8)\text{cm}^{-1}$ . The uncertainty was estimated as the standard error of the fit. Deviation of the VSL data from the theoretical curve for long stripe lengths is due to gain saturation.

Fig. 1b compares the results obtained with the femtosecond VSL to those relating to the integrated SES measurements for the Por-Si sample [7]. Both curves differ significantly. The integrated SES increases sublinearly, as expected, and the estimated optical losses are  $(20 \pm 7)\text{cm}^{-1}$ . Such a behavior rules out possible artifacts influencing the VSL experiment. On the contrary, the VSL curve, plotting the amplified spontaneous emission (ASE) against the length of the excited stripe, exhibits initial exponential increase indicating optical gain, followed by a saturation region. Modal gain, which was obtained as a fitting parameter of the exponential part of the data [2–7], reaches a value of about  $(25 \pm 8)\text{cm}^{-1}$ . The corresponding optical gain spectrum is depicted in Fig. 1a (solid line) showing positive optical gain in the region 570–730nm. The gain spectrum is clearly narrower (FWHM  $\sim 130\text{nm}$ ) and slightly blue-shifted with respect to the normal incidence PL. Similar blue shift of the gain spectrum was also reported in Ref. [4].

Fig. 2 demonstrates the unusual waveguiding properties of the planar waveguide prepared by the Si-ion implantation. PL emission measurement in standard geometry (curve *a*), detected perpendicularly to the waveguide plane, shows a wide emission band in the

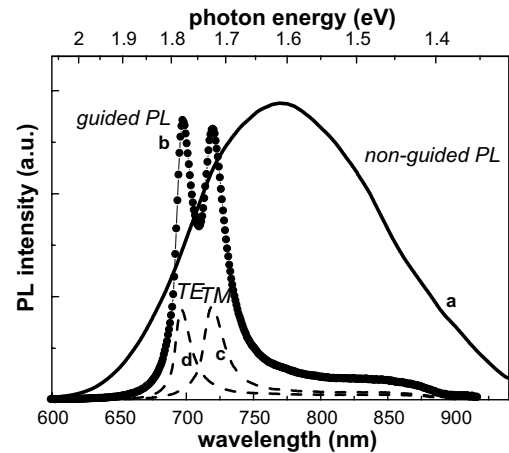


Fig. 2. Photoluminescence spectra of the waveguiding  $\text{Si}^+$ -implanted sample excited by the 325nm line of a He-Cd laser ( $I_{\text{exc}} = 0.26\text{W}/\text{cm}^2$ ). Curves *a* and *b* were detected in directions perpendicular (non-guided, common PL geometry) and parallel (guided, VSL/SES geometry) to the waveguide, respectively. Dashed lines (*c* and *d*) are the polarisation resolved TM and TE modes.

red spectral region 620–950nm. On the contrary, the PL collected from the sample edge (curve *b*) reveals significant PL lineshape narrowing. Splitting of the emission into spectrally resolved TE ( $\sim 695\text{nm}$ ) and TM ( $\sim 720\text{nm}$ ) modes of FWHM  $\sim 20\text{nm}$  is observed, accompanied on the red side by a weak broad unpolarised wing extending to  $\sim 900\text{nm}$ . We have recently suggested an explanation of this peculiar effect in terms of leaky-mode emission localized in the core/substrate interface [12,13]. Such an emission originates from constructive Fabry–Perot interference of the luminescence rays, which are totally reflected at the sample surface back into the active Si-nc layer and emerging at the angle close to the total internal reflection angle in the region near the core/substrate boundary, i.e. in the direction almost parallel to the waveguide plane. The mode splitting is due to polarisation dependent phase-shift introduced during the total reflection at the sample surface. On the other hand, regular guided modes propagating inside the waveguide core are significantly damped due to significant core losses. The originally unresolved broad spectral emission is then strongly suppressed in the PL spectrum recorded from the sample edge, whereas the emission from the leaky modes becomes dominant.

The comparison of the femtosecond VSL and integrated SES data obtained on the waveguiding Si-implanted sample at two different wavelengths, 690nm (TE leaky mode) and 825nm (standard waveguide modes), is shown in Fig. 3. The total matching of the VSL curves with the integrated SES data confirms the absence of nonlinear optical effect, i.e. no optical gain. Both curves show weak losses, which are lower for the wavelength corresponding to the leaky mode. This

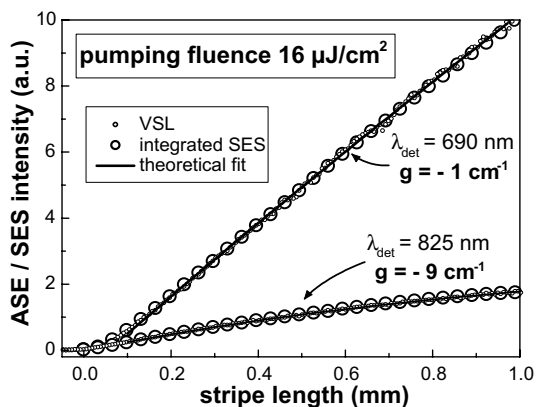


Fig. 3. Femtosecond VSL (small circles) and integrated SES (large circles) measurement on the waveguiding Si<sup>+</sup>-implanted SiO<sub>2</sub> samples. Theoretical fit of the data (full lines) yields losses  $\alpha = 1\text{ cm}^{-1}$  for the detection wavelength  $\lambda_{\text{det}} = 690\text{ nm}$  (TE mode) and  $\alpha = 9\text{ cm}^{-1}$  for  $\lambda_{\text{det}} = 825\text{ nm}$  (ordinary waveguide modes).

observation can be explained by the fact that the leaky modes propagate in the core/substrate region with low density of Si-nc where Mie scattering on coagulated Si-nc and absorption losses are lower. This is in accordance with our previous results obtained using continuous wave VSL measurements [16].

Nanosecond and low repetition rate frequency VSL experiment provides an advantage of achieving higher pumping fluence and time-resolved detection. Time-resolved results obtained by varying the pumping fluence at a fixed pumping length of 1.8 mm are shown in Fig. 4a. While only a slow component (decay time  $\tau \sim 1\ \mu\text{s}$ ) was detected at low intensity, a new fast emission peak ( $\tau \sim 100\text{ ns}$ ), due to stimulated emission [4], appears above a certain pumping threshold of  $\sim 50\text{ mJ/cm}^2$ . Fig. 4b plots the fast emission peak intensity as a function of the stripe length for emission wavelength of 760 nm and for two very different excitation fluences. The sublinear dependence for the fluence of  $5\text{ mJ/cm}^2$  that shows optical losses of  $6\text{ cm}^{-1}$  at low excitation fluence, changes in an exponential increase for the fluence  $86\text{ mJ/cm}^2$ , hence indicating the presence of stimulated emission. The estimated net modal gain is  $12\text{ cm}^{-1}$ . The presence of stimulated emission was further supported by a superlinear fast emission increase above the pumping threshold accompanied by the fast recombination lifetime shortening [16].

The role of the leaky mode emission in the VSL experiment remains to be explained. Intense nanosecond pumping in the VSL experiment produced enough gain in the Si-nc (forming the waveguide core) to overcome waveguide losses. Recently we have tentatively assigned the observed positive gain of  $12\text{ cm}^{-1}$  at 760 nm (Fig. 4b) previously to the TM leaky mode [16]. The results for TE polarisation are not available at the moment. On the other hand, one could expect that the

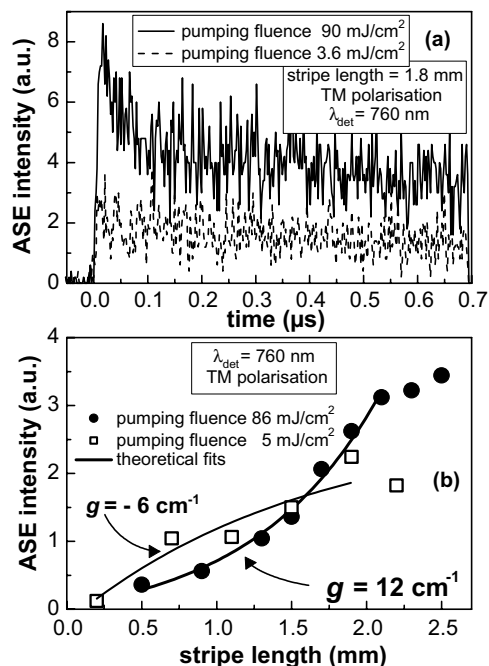


Fig. 4. (a) Time-resolved nanosecond VSL results for the waveguiding Si<sup>+</sup>-implanted SiO<sub>2</sub> sample obtained at  $\lambda_{\text{det}} = 760\text{ nm}$  for pumping fluences of  $86\text{ mJ/cm}^2$  (full line) and  $5\text{ mJ/cm}^2$  (dashed line). Excitation wavelength  $\lambda_{\text{exc}} = 355\text{ nm}$ . (b) Fast component peak intensity as a function of the length of the excited region for two different pumping fluences. Theoretical fit of the data (full line) yields net modal gain value of  $g = (12 \pm 2)\text{ cm}^{-1}$  at a pumping fluence of  $86\text{ mJ/cm}^2$  and a loss value  $\alpha = -g = (6 \pm 6)\text{ cm}^{-1}$  at  $5\text{ mJ/cm}^2$ .

usual waveguide modes will be amplified rather than the leaky modes, where the propagating light leaves the core region within a finite number of total reflections on the core/cladding and core/substrate boundaries and propagates further in the region free from Si-nc. Fig. 5 shows the PL emission spectrum collected from the sample edge with the nanosecond VSL setup.

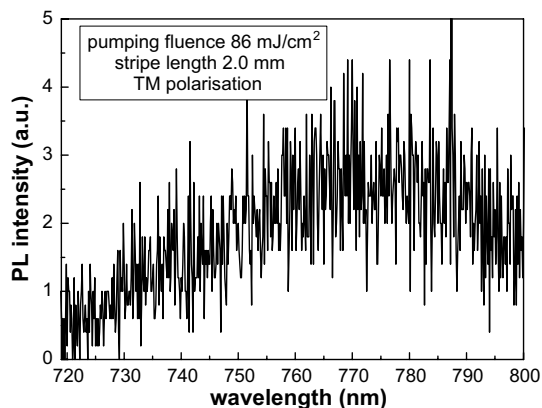


Fig. 5. Edge emission spectrum of the waveguiding Si<sup>+</sup>-implanted SiO<sub>2</sub> sample obtained for stripe length  $l = 2\text{ mm}$  using nanosecond VSL configuration (pumping fluence of  $86\text{ mJ/cm}^2$ ).



Indeed, the broad featureless spectrum resembles strongly the non-guided PL spectrum obtained at normal incidence (compare with solid line in Fig. 2a). In fact both types of modes can contribute to the optical amplification and the insufficient spectral and angular resolutions of the set-up do not enable us to separate reliably their relative contributions. Further fine experiments as well as theoretical modeling are required to elucidate this issue.

#### 4. Discussion

We have observed positive optical gain in both types of samples. However, in Por-Si the pumping fluence needed to achieve stimulated emission is lower. This is probably related to the shorter emission wavelength of Por-Si sample. A decrease in the Si-nc size, linked to the blue shift of the PL, should enhance the probability of the stimulated recombination due to the quantum confinement effect (mixing of quasi-direct transitions). Moreover, the probability of the fast competitive non-radiative processes, such as the free carrier absorption (its cross-section being proportional to  $\lambda^2$ ), is simultaneously reduced [17].

Another advantage of the Por-Si samples is the wide range of the Si-nc concentrations that can be formed (3–45 vol.%), allowing one to prepare samples with high Si-nc density, leading to further blue shift of the PL by filtering the porous silicon particles. Also the presence of phosphorus in the SiO<sub>2</sub> host can play a positive role in the blue shift of the PL emission [18] (see Fig. 1a) and in the passivation of the dangling bonds [19] that act as non-radiative recombination centers. On the other hand, as the Por-Si samples suffer from spontaneous coalescence of the porous silicon powder during preparation, the optical homogeneity and optical quality of the Por-Si samples need improvement.

The high quality of the waveguiding of the Si<sup>+</sup>-ion implanted SiO<sub>2</sub> samples is expected to create, at first sight, much more favorable conditions for the occurrence of the stimulated emission. Although the presence of the leaky modes complicates the interpretation of the VSL data, it seems that it does not prevent achievement of the optical gain at high pump pulsed fluences. The observation of stimulated emission in either “ordinary” waveguide modes or leaky modes, is probably dependent on several experimental parameters. In our particular case, the observed modal gain  $\sim 12\text{ cm}^{-1}$  is lower than that obtained with Por-Si and those reported by other authors [3–7]. This is probably due to both the red-shifted emission in comparison with Por-Si samples and the fact that the excitation energy leaks out step by step from the population-inverted core, which results in lower gain.

#### 5. Conclusions

In conclusion, we have tested the presence of stimulated emission in two different types of Si nanocrystalline samples: a non-waveguiding layer of porous silicon grains embedded in a sol–gel derived SiO<sub>2</sub> matrix and a planar nanocrystalline waveguide prepared by silicon-ion implantation ( $400\text{ keV}$ ,  $4 \times 10^{17}\text{ cm}^{-2}$ ) into a silica substrate. The PL of the ion-implanted sample exhibits polarisation-resolved narrow peaks due to leaky-mode emission. In both types of samples we have observed small optical gain under different pumping conditions (modal gain of  $12\text{ cm}^{-1}$  at  $\sim 760\text{ nm}$  in ion implanted sample and  $25\text{ cm}^{-1}$  at  $\sim 650\text{ nm}$  in sol–gel embedded sample, respectively).

#### Acknowledgements

This work was supported by Projects Nos. 202/01/D030 and 202/03/0789 of GACR, Project No. IAA1010316 of GAAVCR, and by ME 486 of the Ministry of Education CR. The authors thank R. Elliman from Australian National University, Canberra, for providing the samples.

#### References

- [1] For a review on light emission possibilities of silicon, see e.g. D.J. Lockwood *Light Emission in Silicon—From Physics to Devices*, Semiconductors and Semimetals, Vol. 49, Academic Press, San Diego, 1998.
- [2] L. Pavesi, L. Dal Negro, C. Mazzoleni, G. Franzo, F. Priolo, *Nature* 408 (2000) 440.
- [3] L. Dal Negro, M. Cazzanelli, N. Daldosso, Z. Gaburro, L. Pavesi, F. Priolo, D. Pacifici, G. Franzo, F. Iacona, *Physica E* 16 (2003) 297.
- [4] L. Dal Negro, M. Cazzanelli, L. Pavesi, D. Pacifici, G. Franzo, F. Priolo, F. Iacona, *Appl. Phys. Lett.* 82 (2003) 4636.
- [5] L. Khriachtchev, M. Rasanen, S. Novikov, J. Sinkkonen, *Appl. Phys. Lett.* 79 (2001) 1249.
- [6] J. Ruan, P.M. Fauchet, L. Dal Negro, M. Cazzanelli, L. Pavesi, *Appl. Phys. Lett.* 83 (2003) 5479.
- [7] K. Luterová, K. Dohnalová, V. Švrček, I. Pelant, J.-P. Likforman, O. Crégut, P. Gilliot, B. Hönerlage, *Appl. Phys. Lett.* 84 (2004) 3280.
- [8] M.H. Nayfeh, N. Barry, J. Therrien, O. Aksakir, E. Gratton, G. Belomoin, *Appl. Phys. Lett.* 78 (2001) 1131.
- [9] K. Luterová, I. Pelant, I. Mikulskas, R. Tomasiunas, D. Muller, J.-J. Grob, J.-L. Rehspringer, B. Hönerlage, *J. Appl. Phys.* 91 (2002) 2896.
- [10] J. Valenta, I. Pelant, K. Luterová, R. Tomasiunas, S. Cheylan, R.G. Elliman, J. Linnros, B. Hönerlage, *Appl. Phys. Lett.* 82 (2003) 955.
- [11] L. Khriachtchev, M. Räsänen, S. Novikov, *Appl. Phys. Lett.* 83 (2003) 3018.
- [12] J. Valenta, T. Ostatnický, I. Pelant, P. Janda, R.G. Elliman, J. Linnros, B. Hönerlage, *J. Appl. Phys.*, submitted for publication.

- [13] T. Ostatnický, J. Valenta, I. Pelant, K. Luterová, R.G. Elliman, S. Cheylan, B. Hönerlage, *Optical Materials* (2005), these Proceedings.
- [14] J. Valenta, I. Pelant, J. Linnros, *Appl. Phys. Lett.* 81 (2002) 1396.
- [15] V. Švrček, I. Pelant, J.-L. Rehspringer, P. Gilliot, D. Ohlmann, O. Crégut, B. Hönerlage, T. Chvojka, J. Valenta, J. Dian, *Mater. Sci. Eng. C* 19 (2002) 233.
- [16] K. Luterová, D. Navarro, M. Cazzanelli, T. Ostatnický, J. Valenta, S. Cheylan, I. Pelant, L. Pavesi, in: 4th PSSST Conference, Valencia, *Phys. Stat. Sol. C*, submitted for publication.
- [17] W.P. Dumke, *Phys. Rev.* 127 (1962) 1559.
- [18] V. Švrček, A. Slaoui, J.-C. Muller, J.-L. Rehspringer, B. Hönerlage, R. Tomasiunas, I. Pelant, *Physica E* 16 (2003) 420.
- [19] M. Fujii, A. Mimura, S. Hayashi, K. Yamamoto, C. Urakawa, H. Ohta, *J. Appl. Phys.* 87 (2000) 1855.